ACS NANO

www.acsnano.org

ARTICLE

In Vivo Toxicity Assessment of Occupational Components of the Carbon Nanotube Life Cycle To Provide Context to Potential Health Effects

Lindsey Bishop,[†,‡] Lorenzo Cena,[†,§] Marlene Orandle,[†] Naveena Yanamala,[†] Matthew M. Dahm,[∥] M. Eileen Birch,[∥] Douglas E. Evans,[∥] Vamsi K. Kodali,[†] Tracy Eye,[†] Lori Battelli,[†] Patti C. Zeidler-Erdely,[†] Gary Casuccio,[⊥] Kristin Bunker,[⊥] Jason S. Lupoi,[⊥] Traci L. Lersch,[⊥] Aleksandr B. Stefaniak,[†] Tina Sager,[†] Aliakbar Afshari,[†] Diane Schwegler-Berry,[†] Sherri Friend,[†] Jonathan Kang,[‡] Katelyn J. Siegrist,[†] Constance A. Mitchell,[†] David T. Lowry,[†] Michael L. Kashon,[†] Robert R. Mercer,[†] Charles L. Geraci,[∥] Mary K. Schubauer-Berigan,[∥] Linda M. Sargent,[†] and Aaron Erdely*[,†,‡]

[†]National Institute for Occupational Safety and Health, Morgantown, West Virginia 26505, United States

[‡]West Virginia University, Morgantown, West Virginia 26505, United States

[§]West Chester University, West Chester, Pennsylvania 19383, United States

[∥]National Institute for Occupational Safety and Health, Cincinnati, Ohio 45213, United States

[⊥]RJ Lee Group, Monroeville, Pennsylvania 15146, United States

Supporting Information

ABSTRACT: **Pulmonary toxicity studies on carbon nanotubes focus primarily on as-produced materials and rarely are guided by a life cycle perspective or integration with exposure assessment. Understanding toxicity beyond the as-produced, or pure native material, is critical, due to modifications needed to overcome barriers to commercialization of applications. In the first series of studies, the toxicity of as-produced carbon nanotubes and their polymer-coated counterparts was evaluated in reference to exposure assessment, material characterization, and stability of the polymer coating in biological fluids. The second series of studies examined the toxicity of aerosols generated from sanding polymer-coated carbon-nanotube-embedded or neat composites. Postproduction modification by polymer coating did not enhance pulmonary injury, inflammation, and pathology or *in vitro* genotoxicity of as-produced carbon nanotubes, and for a particular coating, toxicity was significantly attenuated. The aerosols generated from sanding composites embedded with polymer-coated carbon nanotubes contained no evidence of free nanotubes. The percent weight incorporation of polymer-coated carbon nanotubes, 0.15% or 3% by mass, and composite matrix utilized altered the particle size distribution and, in certain circumstances, influenced acute *in vivo* toxicity. Our study provides perspective that, while the number of workers and consumers increases along the life cycle, toxicity and/or potential for exposure to the as-produced material may greatly diminish.**

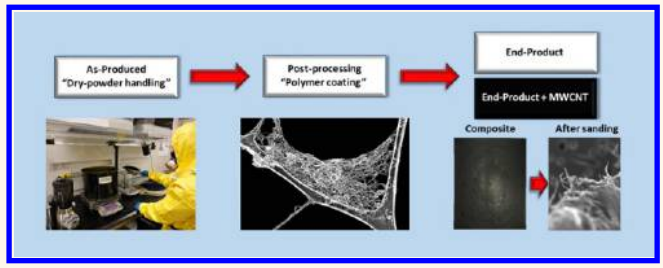

KEYWORDS: *life cycle, carbon nanotubes, exposure assessment, toxicity, composite, polymer coating, genotoxicity*

The potential for human toxicity of many engineered nanomaterials is surmised mostly from laboratory studies on as-produced (pure or pristine) forms. Unfortunately, little attention has been given to incorporating exposure assessment or a life cycle perspective (Supplemental Figure 1) in toxicity study design or outcomes.[1,2] Specifically, extrapolations of dose−response relationships from *in vivo* studies to human health, in the context of exposure assessment, are lacking, especially as a particular engineered nanomaterial proceeds along the product value chain. Also, descriptions of toxicities associated with postproduction modifications of as-produced materials or the aerosols generated from manipulat-

Received: May 3, 2017
Accepted: July 31, 2017
Published: July 31, 2017

DOI: 10.1021/acsnano.7b03038
ACS Nano 2017, 11, 8849−8863

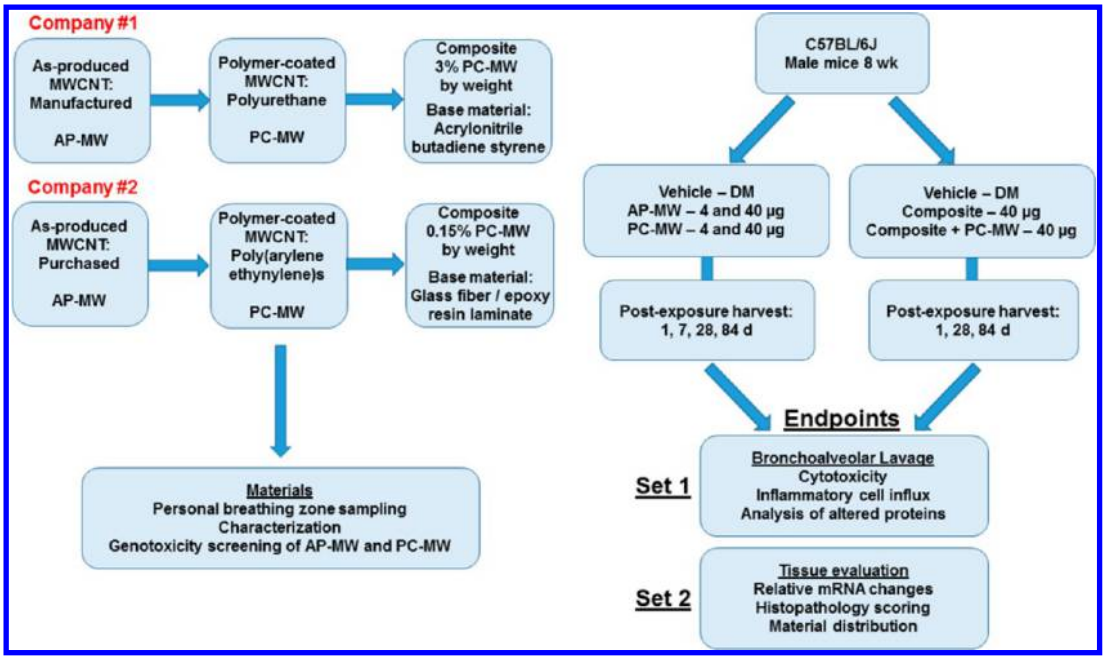

Figure 1. Experimental design to encompass an occupational life cycle perspective. Materials including an as-produced multiwalled carbon nanotube (AP-MW), the polymer-coated counterpart (PC-MW), a composite test sample consisting of the base material only, and a composite test samples with PC-MW were obtained from two separate companies. Materials were characterized, prepared for *in vivo* studies in comparison to ongoing exposure assessment studies, and AP-MW and PC-MW materials were screened for genotoxicity. For *in vivo* studies, male C57BL/6J mice were exposed by oropharyngeal aspiration as indicated and sacrificed 1, 7, 28, and 84 days postexposure to measure the designated end points. The test composites were sanded, and the respirable particulate was collected for *in vivo* exposures.

ing engineered nanomaterial-enabled applications (*e.g.*, composites) are scarce.

Why is the life cycle perspective critical for toxicity studies of engineered nanomaterials? For illustration, consider carbon nanotubes (CNTs). Despite adverse implications from toxicity studies, CNT production continues to increase, and commercialization is progressing for CNT-enabled products (Lux Research, Inc. August 2016; Future Markets, Inc. January 2016). With inhalation as the primary route of occupational exposure, *in vivo* study outcomes after as-produced CNT exposures included pleural penetrations with potential carcinogenicity and mesothelioma, fibrosis, systemic inflammation, neuroinflammation, and immunosuppression.[3−13] In fact, some widely studied CNTs, multiwalled CNT-7 (MWCNT-7) and Baytubes, are no longer in production. While it is difficult to quantify the impact toxicity studies have had on the application of CNTs in industry, environmental health and safety is a justifiable concern during commercialization as the numbers of workers and consumers making or using nanomaterial-enabled products increases along the life cycle vis-à-vis the number of individuals producing and handling the as-produced material.

The aim of this study was to utilize an *in vivo* toxicity assessment of occupational components of the life cycle to evaluate areas of exposure, correlate that evaluation with current material hazard information, and develop a profile that represents the growing applications of CNTs in industry to provide a realistic characterization of possible human health outcomes and guide risk management practices. To accomplish this goal, MWCNT was used as a model engineered nanomaterial for several reasons: (1) CNTs represent a significant market share for engineered nanomaterials with MWCNTs being the majority of that market;[14] (2) MWCNTs represent a highly visible material due to potential for significant pulmonary toxicity;[15−17] (3) extensive exposure assessment has been performed to integrate into toxicity study design and interpretations;[14,18] and (4) companies could provide an as-produced MWCNT, the postproduction modified counterpart, as well as the test composites made with the modified MWCNT to systematically address the potential for toxicity during occupational components of the life cycle.

As-produced MWCNTs (AP-MW), postproduction modified MWCNT counterparts, and aerosols generated from industrial sanding scenarios of postproduction modified MWCNT-enabled composites were evaluated in the current study. The postproduction modification was a polymer coating. Various means to functionalize MWCNTs, including nitrogen-doped, hyaluronic acid, cationic (carboxylate), anionic (amine), or polyethylene glycol, can alter pulmonary toxicity.[19−21] With the largest market for MWCNTs being incorporation into composites, companies are exploring the use of polymer coatings. The polymer coating can be specifically formulated to add stability and increase performance of the final product while minimizing the percent by weight MWCNT incorporation. In some cases, the coating also permits ease of handling and can decrease the dustiness of bulk CNT powders, thereby reducing potential inhalation exposures in downstream applications. The polymer-coated MWCNTs (PC-MW) were then incorporated into distinct composite matrices. The formed composites undergo industrial processes (*e.g.*, sanding) which can lead to human exposures directly or secondarily *via* product handling or environmental accumulation. Characterizing and understanding toxicities of the aerosols generated during processing of nanoenabled composites gives perspective to the potential health effects to workers and, subsequently, to consumers.

DOI: 10.1021/acsnano.7b03038
ACS Nano 2017, 11, 8849−8863

Material	Mean Length μm ± GSD (Range – μm)	Mean Diameter μm ± GSD (Range – μm)	Zeta Potential (mV)	Metal Catalyst	Surface Area (m^2/g)	Density g/cm^3 ± SD	Dustiness Total %	Dustiness Respirable %
Company 1 AP-MW	1.38 ± 2.32 (0.22-50.9)	0.014 ± 1.575 (0.006-0.216)	-12.1±0.6	1.7 % Iron	212	0.087 ± 0.000	2.9	1.1
Company 1 PC-MW	1.17 ± 2.49 (0.01-8.5)	0.014 ± 1.589 (0.006-0.283)	-11.9±0.5	1.7 % Iron	140	0.156 ± 0.003	0.3	0.1
Company 2 AP-MW	1.01 ± 2.00 (0.10-8.5)	0.020 ± 1.695 (0.008-0.275)	-11.1±0.6	2 % Aluminum 1.7 % Iron	219	0.007 ± 0.000	0.3	0.2
Company 2 PC-MW	0.67 ± 1.72* (0.15-2.4)	0.015 ± 1.254 (0.009-0.320)	-10.7±0.4	2 % Aluminum 1.7 % Iron	139	0.103 ± 0.002	3.5	1.1

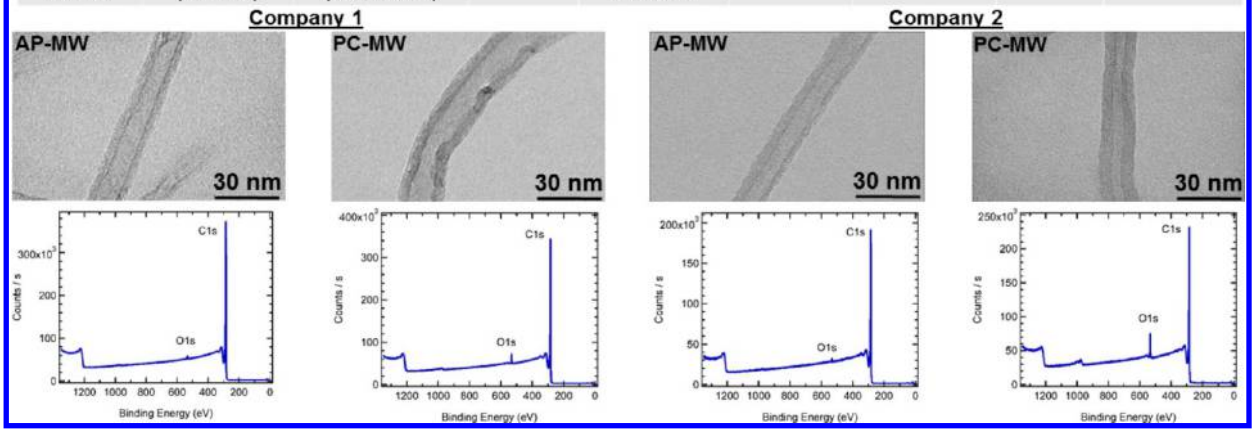

Figure 2. Characterization of materials. Polymer coating affected measurements of length, surface area, density, and dustiness (table). Representative high-resolution electron microscopy images of single tubes show the relative consistency of diameter (middle panels) irrespective of coating. The bottom panels show the increased oxygen content (company 1 O1s 0.88% AP-MW and 2.65% PC-MW; company 2 O1s 1.02% AP-MW and 5.96% PC-MW) measured by X-ray photoelectron spectroscopy in the polymer-coated materials in comparison to the respective AP-MW. The Kolmogorov–Smirnov two-sample test was used to compare the length distributions (*$p < 0.05$ *vs* respective AP-MW).

RESULTS AND DISCUSSION

Materials, described extensively in the Materials and Methods, from two separate companies were evaluated (Figure 1). The first series of studies examined whether the toxicity of AP-MW was altered as a result of polymer coating. The polymer coatings were a polyurethane and a proprietary poly(arylene ethynylene) and were 7 and 15% of the total mass, respectively. The second series of studies examined the characteristics and potential for toxicity of the aerosol generated following sanding of composites containing PC-MW. The MWCNTs utilized were approximately 14 nm in diameter (Figure 2; Supplemental Figure 2). The average length and surface area was slightly reduced with polymer coating, while the density was increased (Figure 2). Chemical bonding consistent with the polymer coating was identified by X-ray photoelectron spectroscopy (Figure 2; Supplemental Figure 2). Diameter was generally unaffected by polymer coating as the range of diameter of the MWCNTs (Supplemental Figure 2) was greater than what would be expected from the coating, given an organic polymer coating can be as thin as 1 nm. Calculations using surface area (Figure 2), mass of the coating, and an assumed density of 1.15 g/cm^3 for the polymer coatings predict a range of 0.4–0.9 nm thickness for the coatings. ζ-Potential and catalytic metal composition were not different due to polymer coating, and endotoxin levels were below level of detection for all materials. Dustiness, the ability of a powder to form an airborne dust by mechanical stimulus, was relatively low for these materials when compared to other nanoscale powders (0.3–3.5% of the total mass).[22] The polymer coating from company 1 reduced dustiness by an order of magnitude (Figure 2). This was expected given the large aggregate nature of the material (described later in Figure 4). Interestingly, dustiness was increased with the proprietary polymer coating from company 2. It is likely the proprietary coating interferes with the attractive forces of the AP-MW. This was not entirely unique as dustiness was increased for other nanoscale materials following surface coating.[23]

Given the potential for inhalation of the PC-MW, stability of the polymer coating on the MWCNT *in vivo* was unknown. Inhaled MWCNTs can be phagocytized by macrophages and compartmentalized in lysosomes, an environment with a pH of 4.5, for programmed degradation.[2,24] MWCNTs can also enter the pulmonary interstitium, inducing alveolar fibrosis.[25] To mimic these *in vivo* settings, PC-MW were incubated in artificial lysosomal fluid (ALF) or interstitial fluid (Gamble's) for up to 21 days (Figure 3; Supplemental Figure 3). Incubations in biological fluids resulted in increased oxygen incorporation (Figure 3a; Supplemental Figure 3) or similar oxygen incorporation but with a shift toward increased carbonyl groups (Figure 3c; Supplemental Figure 3). The oxidation of MWCNTs was expected and has been previously demonstrated using other oxidizing agents.[26–28] The Raman spectral analysis for company 1 (Figure 3b; Supplemental Figure 3) indicated no evidence that the coating was removed during the incubations in the artificial solutions by the lack of any corresponding wavenumber shift in the vibrational modes, consistent with previous findings.[29] For company 2, the Raman analysis of the proprietary coating indicated several characteristics peaks including a strong peak at 2185 cm^{-1} (Figure 3d; Supplemental Figure 3). The peaks associated with the proprietary coating were maintained in all incubation scenarios (Figure 3d; Supplemental Figure 3). The combined XPS and Raman data

DOI: 10.1021/acsnano.7b03038
ACS Nano 2017, 11, 8849–8863

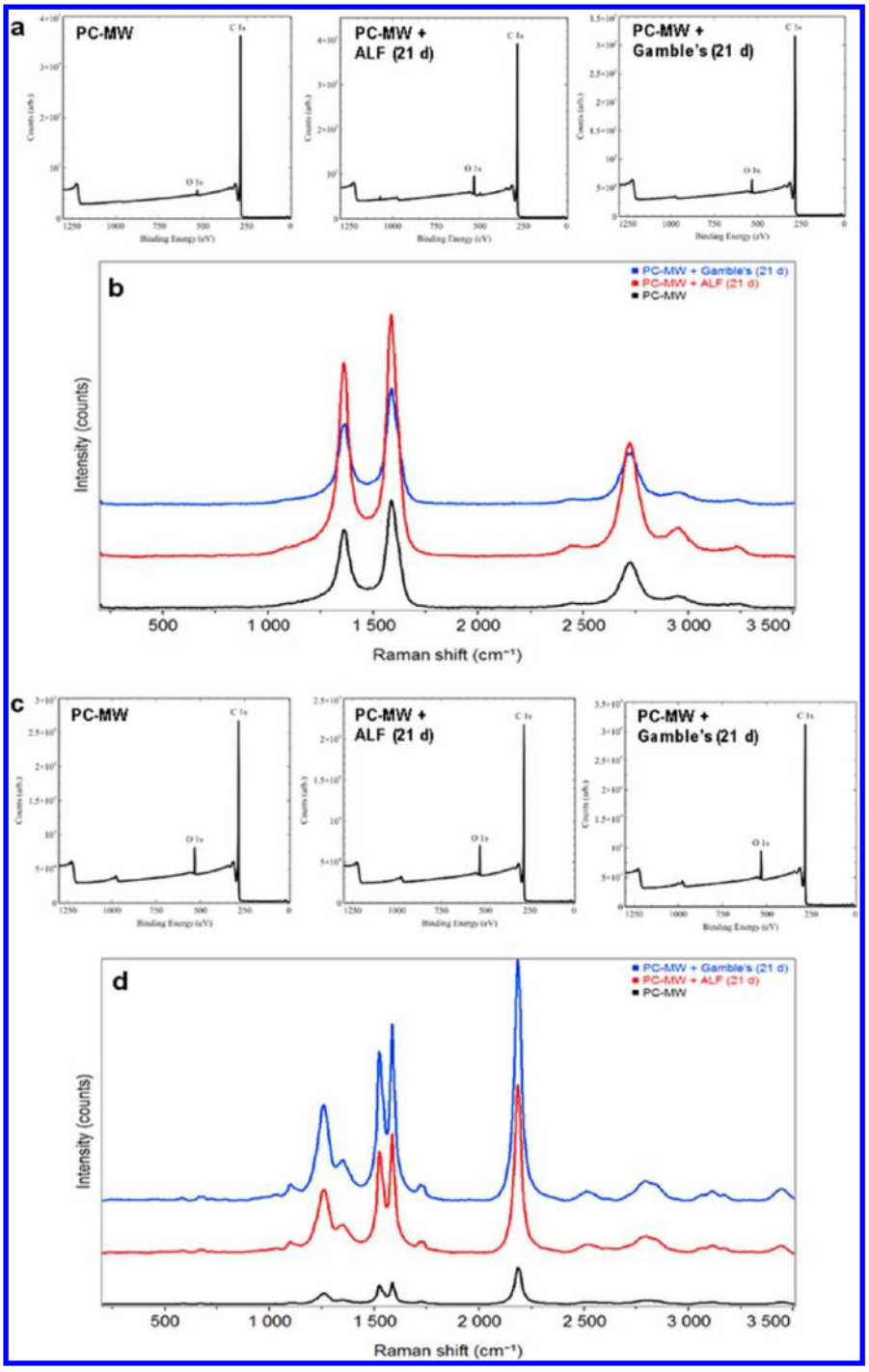

Figure 3. Stability of polymer coating in artificial biological solutions. Polymer-coated MWCNT from company 1 (a,b) and company 2 (c,d) were incubated for 21 days in artificial lysosomal fluid (ALF) or artificial interstitial fluid (Gamble's). (a,c) Total oxygen content was increased (a) or similar (c) following incubations in artificial biological solutions as measured by X-ray photoelectron spectroscopy. (b) Raman spectra analysis indicated no evidence the polymer coating was displaced from the MWCNT from company 1. (d) Spectra analysis from company two clearly indicated a primary polymer peak at 2185 cm^{-1} remained prevalent following incubations up to 21 days.

suggest some oxidation consistent with previous studies and no obvious effects on the stability of the polymer coatings from the experimental conditions to mimic *in vivo* scenarios.

For evaluation of *in vivo* toxicity, initially comparing the AP-MW and their PC-MW counterpart, male C57BL/6J mice were exposed by oropharyngeal aspiration to 4 and 40 μg of the as-produced or polymer-coated MWCNTs, with the weight percent of the coating taken into account. The relevance of the doses used were based on exposure assessment from eight different MWCNT facilities.[1,14,30] The high dose of 40 μg is a well-characterized deposition known to induce pulmonary pathology.[4,17] The lower dose, predicted to represent approximately 7.6 years at average workplace exposure levels,[14] was more representative of the potential cumulative exposure of the current industry.[1,14,30] The extrapolations assume a respirable fraction arithmetic mean of about twice the NIOSH recommended exposure limit (REL) of 1 $\mu g/m^3$. Various end points of pulmonary inflammation, material

DOI: 10.1021/acsnano.7b03038
ACS Nano 2017, 11, 8849–8863

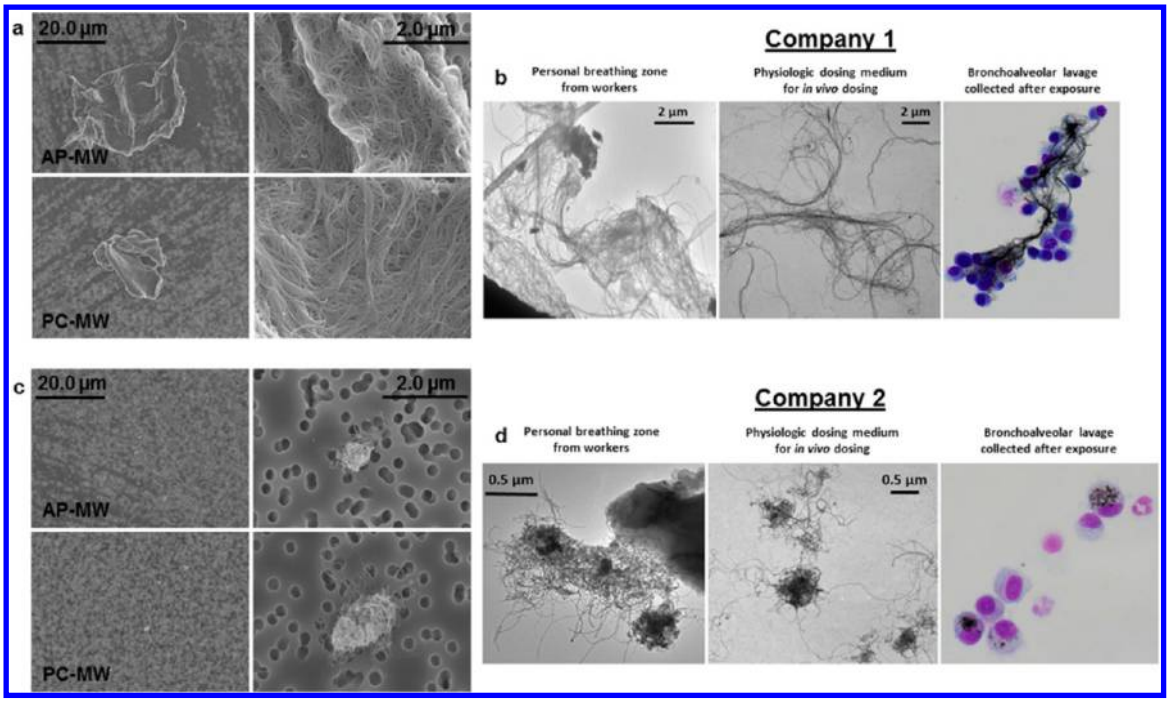

Figure 4. Particle preparations to match occupational settings. (a) Representative scanning electron microscopy images of materials from company 1 (a) and company 2 (c). (b,d) Transmission electron micrographs illustrate consistency between personal breathing zone collections and material preparation in physiologic dosing medium (DM) for *in vivo* dosing. A representative image of the material obtained from the lung by bronchoalveolar lavage (BAL) after exposure showed that the particle morphology was maintained. The representative example for company 1 (b) was for the PC-MW material and for company 2 (d) was the AP-MW material.

distribution in the lung, and histopathology were evaluated 1, 7, 28, and 84 days postexposure (Figure 1). Micronuclei formation, an initial screen for genotoxicity, was determined in immortalized and primary lung epithelial cells.[31]

Generating a dispersed, respirable MWCNT aerosol that can reach the pulmonary alveolar/gas-exchange region was warranted for *in vivo* studies in order to identify adverse effects and contribute to development of a REL. In contrast, facility exposures consist mostly of agglomerated MWCNTs which can be inhaled, and in some instances, only a small fraction is respirable.[18] As such, these MWCNTs can deposit mostly in the conducting, nonalveolar airways.[18] As a primary goal, material preparations used for our *in vivo* studies resembled samples collected from personal breathing zones of workers (Figure 4b,d). While critical for interpretation of human relevance, this distinctive comparison is mostly unavailable or overlooked for toxicity assessments of engineered nanomaterials. Extensive dispersion of agglomerates, especially for the material represented in Figure 4a,b would have resulted in the assessment of a nonrepresentative exposure.

Despite relatively similar diameters of the MWCNTs utilized by the two companies, vastly different agglomerates were observed. Company 1, by design, manufactures a highly entangled cross-linked, or branched, MWCNT that was subsequently spray-coated with a commercial polyurethane. The "branched" MWCNT was synthesized specifically to be large agglomerates (Figure 4a,b) to limit the respirability of the material. In fact, facility exposure assessment of workers indicated that less than 10% of the inhalable fraction of the material was respirable.[18] This is consistent with two-dimensional sizing of the largest crosswise diameter using scanning electron microscopy images (Figure 4a; n = 75 for each represented as geometric means (μm) ± geometric standard deviation; 32.47 ± 1.38 AP-MW *vs* 21.69 ± 1.29* PC-MW; *p < 0.05). In contrast, the agglomerates of MWCNTs from company 2 were much smaller (Figure 4c; 0.77 ± 1.75 AP-MW *vs* 1.01 ± 1.85* PC-MW; p < 0.05) and exposure assessment indicated 40−50% of the inhalable fraction was respirable for facility workers.[18]

The AP-MW from company 1 induced dose-dependent pulmonary cytotoxicity, measured as lactate dehydrogenase levels in the bronchoalveolar lavage fluid, which resolved with time (Figure 5a). Influx of polymorphonuclear cells, representing pulmonary inflammation, peaked at 1 day postexposure (Figure 5b; Supplemental Table 1). Macrophage influx was prominent 7 days postexposure and resolved by 84 days postexposure (Figure 5b; Supplemental Table 1). A panel of proteins, measured in the bronchoalveolar lavage fluid at 1 and 28 days postexposure, and relative mRNA expression, measured in lung tissue, related primarily to the innate inflammatory response, were elevated mostly at 1 day postexposure (Figure 5c; Supplemental Figure 4; Supplemental Tables 2 and 3). Polymer coating (polyurethane spray coating) the AP-MW did not alter lung injury or the inflammatory response. Although there was no difference in the described inflammatory parameters at an equal mass basis, it should be noted that the polymer coating reduced the dustiness of the material by 10-fold.

Exposure assessment studies in company 1[18] indicated the respirable fraction was below the NIOSH REL of 1 $\mu g/m^3$ elemental carbon as a respirable mass 8 h time-weighted average concentration while the average inhalable fraction was greater than 10 $\mu g/m^3$. With only a small percentage of the inhalable fraction being respirable, epidemiologists inquired about the health outcomes of the inhalable fraction. Our facility-representative material preparation resulted in the

DOI: 10.1021/acsnano.7b03038
ACS Nano 2017, 11, 8849−8863

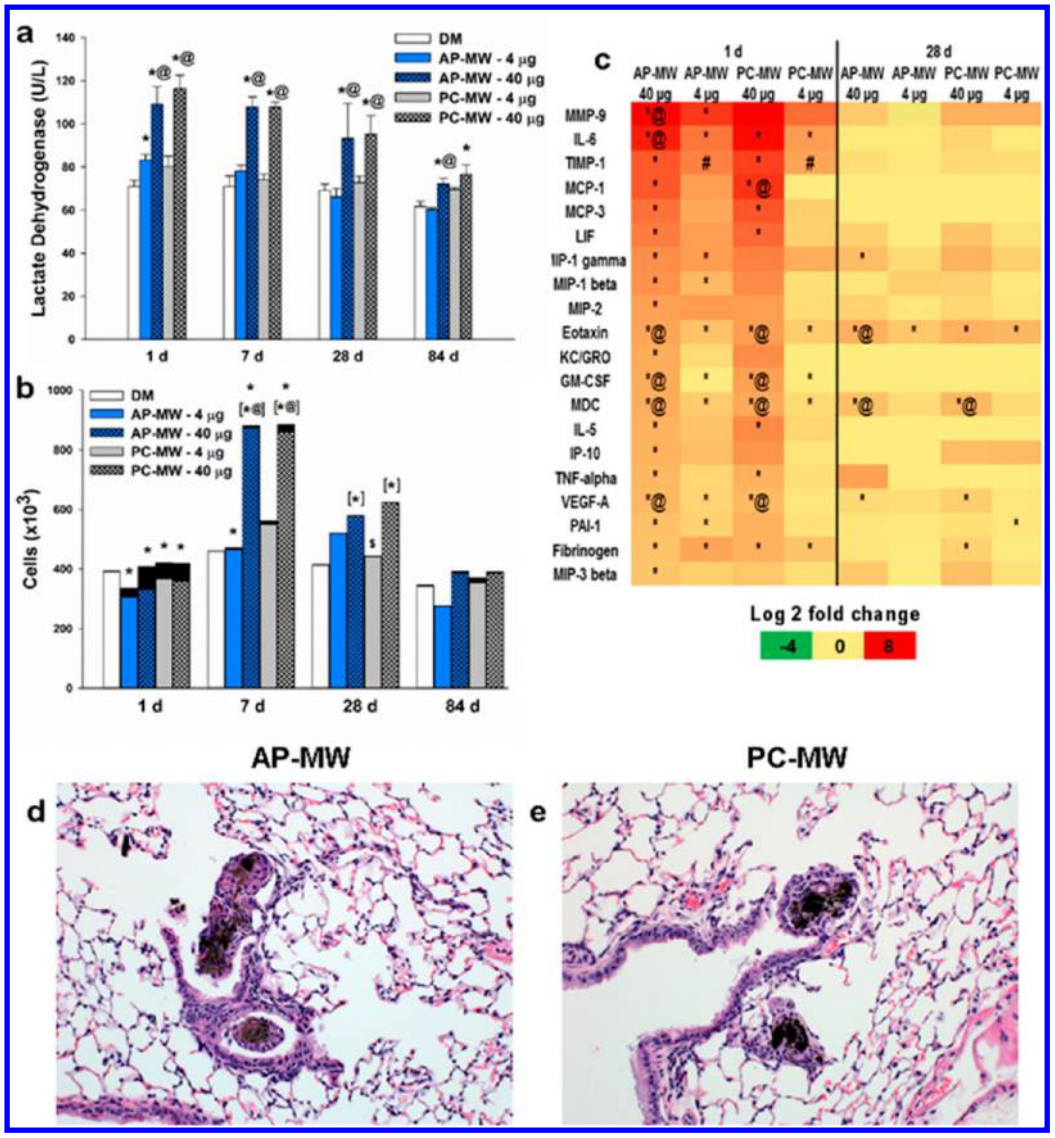

Figure 5. Pulmonary injury, inflammation, and pathology induced by as-produced MWCNTs (AP-MW) and polymer-coated counterpart (PC-MW) from company 1. (a–c) Pulmonary cytotoxicity (a), inflammatory cell influx (b; macrophages represented by open bars with or without cross-hatch and polymorphonuclear cells represented by solid black bars), and inflammatory proteins measured in BAL fluid (c) were increased due to exposure and resolved with time. Similar effects were observed following exposure to AP-MW when compared to PC-MW. (d,e) Similarity existed in the pathological responses induced by AP-MW (d) or PC-MW (e) in the 40 μg exposure groups. *$p < 0.05$ *vs* DM; #$p < 0.05$ *vs* all groups at a given time point; @$p < 0.05$ *vs* 4 μg of same material; \$$p < 0.05$ *vs* AP-MW of equal dose. Analyses were performed by a two-way factorial analysis of variance or nonparametric Kruskal–Wallis tests for each postexposure time point, and pairwise comparisons were generated using the Dwass, Steel, Critchlow–Fligner method. Brackets around significance symbols (b) represent macrophages, and symbols without brackets represent polymorphonuclear cells.

majority of particles depositing in the conducting airways, not in the alveolar region (Supplemental Figure 5), consistent with the exposure assessment findings. There was 50–75% clearance of material from the nonalveolar, airway region by 84 days, but what remained induced proliferative bronchiolitis obliterans (Figure 5d,e). Proliferative bronchiolitis obliterans is a condition resulting from epithelial cell injury and aberrant tissue repair.[32] Incidence was high in the 40 μg dose groups, irrespective of whether the polymer coating was present, but it was also observed in one animal of each of the 4 μg groups. This suggests the toxicity was more associated with the relatively large agglomerate size and conducting airway deposition than potential effects due to polymer coating (Supplemental Table 4). It is unknown if the same deposition, retention, and histopathology would result in exposed humans. Currently, the NIOSH REL is based on development of lung effects (*e.g.*, fibrosis) of a respirable fraction.[33] Additional considerations may be warranted in situations where exposures are disproportionately inhalable.

Company 2 applied a proprietary poly(arylene ethynylene) coating bound by π-stacking to a commercially available MWCNT, the Graphistrength C100 produced by Arkema. The coating consists of the polymer backbone adsorbed along the side walls of the MWCNTs by π-stacking with specific organic side chains attached to the backbone similar, but not the same as the coating analyzed by Chen *et al.*[34] While similar in diameter to that of company 1, personal breathing zone sampling illustrated a vastly different agglomerated particle that macrophages could internalize (Figure 4c,d), consistent with deeper lung penetration (Supplemental Figure 5) and ongoing

DOI: 10.1021/acsnano.7b03038
ACS Nano 2017, 11, 8849–8863

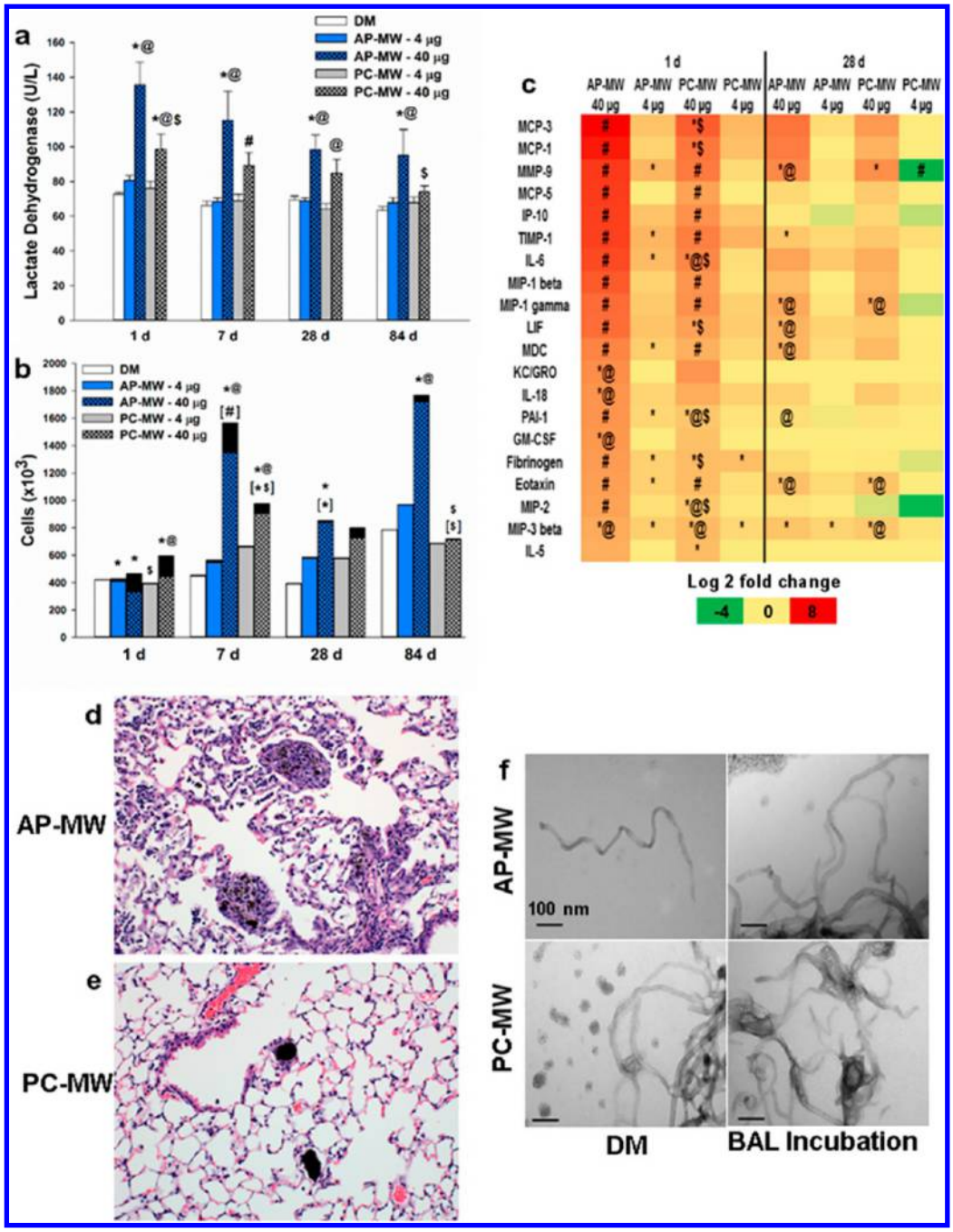

Figure 6. Pulmonary injury, inflammation, pathology, and autoagglomeration induced by as-produced MWCNT (AP-MW) and polymer-coated counterpart (PC-MW) from company 2. (a–c) Pulmonary cytotoxicity (a), inflammatory cell influx (b; macrophages represented by open bars with or without cross-hatch and polymorphonuclear cells represented by solid black bars), and inflammatory proteins measured in BAL fluid (c) were increased due to exposure and resolved with time. In comparison to AP-MW, effects were significantly attenuated in mice exposed to PC-MW. (d) Granulomas were observed in the AP-MW mice exposed to 40 μg. (e) Agglomerates of particles without noticeable surrounding inflammation were observed in mice exposed to 40 μg of PC-MW. (f) Physiologic dosing medium (DM), used to prepare the MWCNT for *in vivo* dosing, did not interact with the surface of the PC-MW (bottom left inset) similarly to the AP-MW (upper left inset) resulting in increased agglomeration of PC-MW materials when incubated *ex vivo* with collected mouse bronchoalveolar lavage fluid (lower right inset). *$p < 0.05$ *vs* DM; #$p < 0.05$ *vs* all groups at a given time point; @$p < 0.05$ *vs* 4 μg of same material; \$$p < 0.05$ *vs* AP-MW of equal dose. Analyses were performed by a two-way factorial analysis of variance or nonparametric Kruskal–Wallis tests for each postexposure time point, and pairwise comparisons were generated using the Dwass, Steel, Critchlow–Fligner method. Brackets around significance symbols (b) represent macrophages, and symbols without brackets represent polymorphonuclear cells.

exposure assessments. The as-produced material from company 2 induced dose-dependent cytotoxicity and inflammation that resolved with time (Figure 6a–c; Supplemental Figure 6; Supplemental Tables 5–7). Interestingly, these effects were attenuated significantly in mice exposed to the polymer-coated counterpart, which complemented previous results of a polystyrene-coated MWCNT.[35] The as-produced MWCNT used for the polystyrene-coating was from Arkema, suggesting

DOI: 10.1021/acsnano.7b03038
ACS Nano 2017, 11, 8849–8863

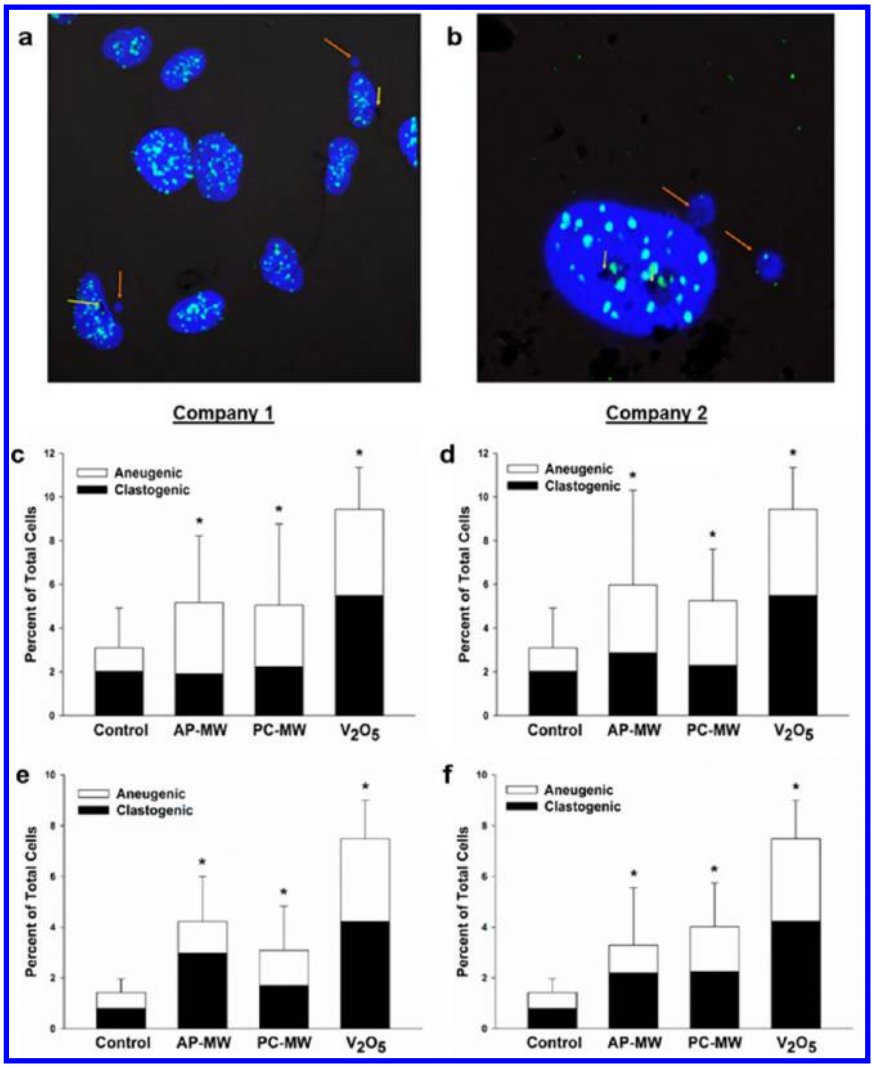

Figure 7. Evaluation of micronuclei, an initial screen for genotoxicity, in immortalized (BEAS-2B) or primary small airway epithelial cells (SAEC) exposed to AP-MW or PC-MW. Micronuclei enumeration was used to analyze either (a) centromere positive (chromosome loss) or (b) centromere negative (chromosome breakage), as shown in the representative images. All MWCNTs produced significantly greater amounts of micronuclei in both the BEAS-2B (c,d) and the SAEC (e,f) cells following exposure to 2.4 μg/mL MWCNT. Vanadium pentoxide (V_2O_5) at 3.2 μg/mL was used as a positive control. A pancentromere stain was used to determine type of DNA damage, either clastogenic (black bars) or aneugenic (white bars).

some physicochemical similarities and/or pulmonary handling to the coated material from company 2. Granuloma formation was more prominent in the as-produced MWCNT-exposed mice (Figure 6d, Supplemental Table 4). That was consistent with the lack of osteopontin expression, a mediator necessary for granuloma formation,[36,37] in the PC-MW group (Supplemental Figure 6). In the PC-MW-exposed mice, agglomerates, although few, were consistently present and seemingly unrecognized by inflammatory cells (Figure 6e). The outcome was unexpected, and we hypothesized that the agglomeration could be a consequence of the polymer coating modulating differential interactions with surfactant layer components potentially increasing adhesion and culminating in autoagglomeration of PC-MW.[38] This was also illustrated by particle incubation with collected murine lavage fluid (Figure 6f). AP-MW prepared in the physiologic dispersion media was subsequently incubated in collected bronchoalveolar lavage fluid resulting in the adsorption or coating of lipids and/or albumin on the surface of MWCNTs (Figure 6f). However, for PC-MW, differential interactions or inefficient coating of lung surfactant or dispersion media components on the surface, likely due to the presence of polymer-coating, resulted in the agglomeration of particles (Figure 6f). The fate and persistence of the agglomerates is unknown, but presence only in the 40 μg exposure group, a dose predicted to exceed occupational exposures,[14] suggests that deposited dose was a factor.

As an initial screen for genotoxicity and influence of the polymer coatings, micronuclei were enumerated. Significantly increased micronuclei were evident in immortalized (Figure 7c,d) and cultured primary lung epithelial (Figure 7e,f) cells following exposure to 2.4 μg/mL AP-MW or PC-MW from companies 1 and 2. Both chromosome negative (Figure 7a) and chromosome positive micronuclei (Figure 7b) were observed, indicating that CNT-induced genetic damage was due to chromosome breakage (clastogenicity) as well as errors in chromosome number (aneuploidy). The data demonstrating increased aneuploidy suggest disruption of the mitotic spindle. Indeed, previous investigations have shown that exposure to a MWCNT of similar diameter caused disruption of the division apparatus, which resulted in loss and gain of chromosomes.[31,39]

DOI: 10.1021/acsnano.7b03038
ACS Nano 2017, 11, 8849–8863

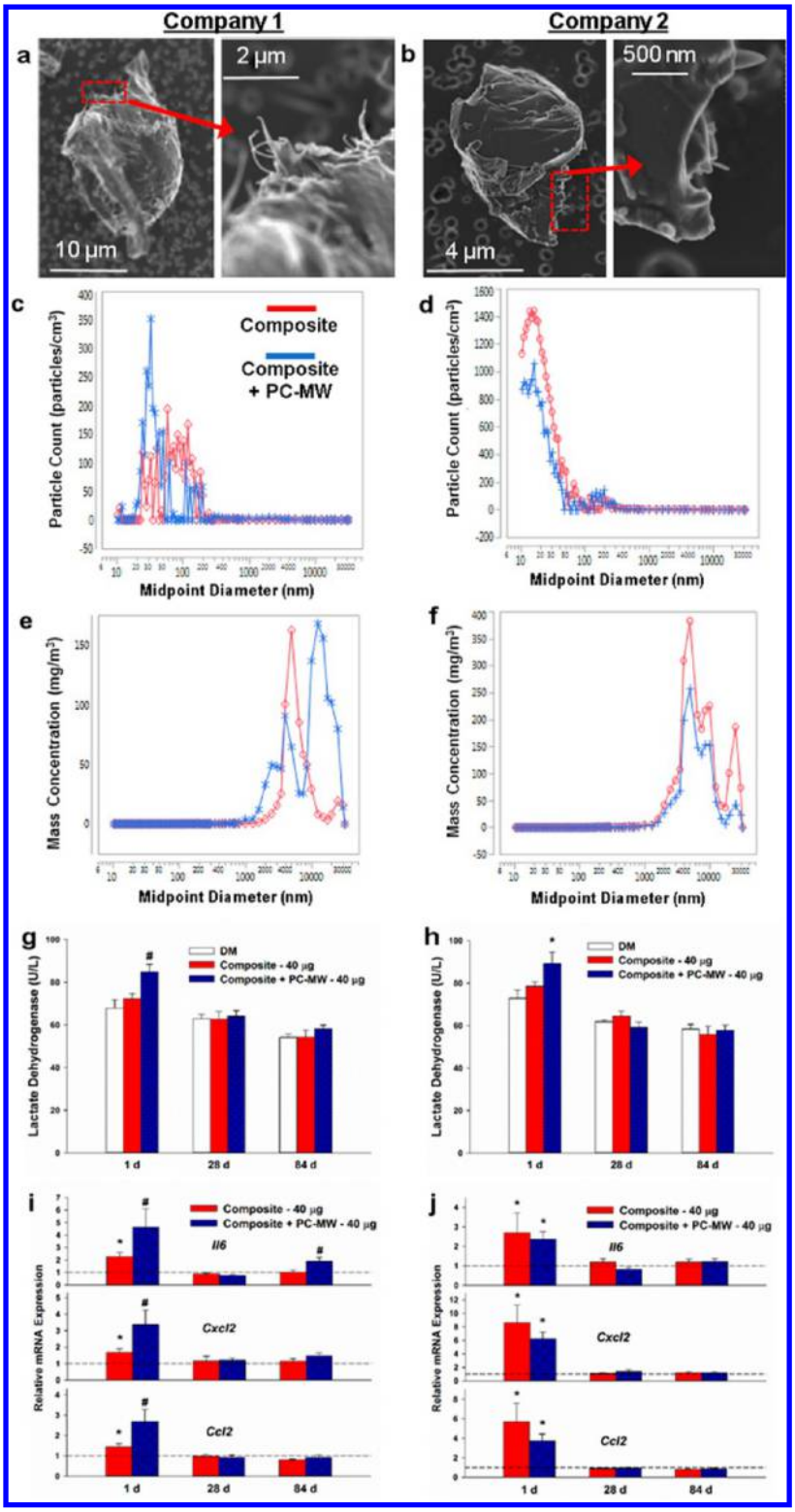

Figure 8. Aerosol characteristics and toxicity from respirable particles generated following sanding composites and composites containing polymer-coated MWCNT (PC-MW). (a,b) Representative images collected from composites + PC-MW. Protrusions of PC-MW were consistent with the percent loading; 3% for company 1 and 0.15% for company 2. (c–f) Size distribution by particle count (c,d) and mass concentration (e,f) were shifted due to PC-MW loading in company 1 but not for company 2. (g,i) Pulmonary cytotoxicity (g) and inflammatory relative mRNA expression (i) were acutely increased in the composite + PC-MW from company 1 compared to composite group alone. (h) Pulmonary cytotoxicity was increased in the composite + PC-MW group from company 2 but was not different from composite alone. (j) Inflammatory relative mRNA expression was similarly increased acutely in the composite and composite + PC-MW groups. *$p < 0.05$ *vs* DM; #$p < 0.05$ *vs* all groups at a given time point. Analysis were performed by a two-way factorial analysis of variance or nonparametric Kruskal–Wallis tests for each postexposure time point, and pairwise comparisons were generated using the Dwass, Steel, Critchlow–Fligner method. The reference line (i,j) represents the sham group.

DOI: 10.1021/acsnano.7b03038
ACS Nano 2017, 11, 8849–8863

Because the polymer coating did not alter either the percent of CNT-induced aneuploidy or clastogenicity (Figure 7c–f), the data further indicate that the physical properties of the CNT structure were responsible for the genotoxic response. While the effects were based on equal mass *in vitro*, we again note that company 1 reduced dustiness by 10-fold, and for company 2, inflammation, a risk factor for cancer progression,[40] was significantly attenuated *in vivo* with polymer coating.

Composites, some of the largest commercialization end products for MWCNTs, were the primary downstream application for the PC-MW. Initial studies examining CNT-enabled composites have shown no release of unbound CNTs following cutting or sanding, while others suggest potential release.[41−46] Results were dependent on matrix and percent mass loading of the CNTs. We developed a system to mimic industrial scenarios (*e.g.*, sanding, cutting) that would allow a standardized approach to generate and characterize the aerosols generated from CNT-enabled composites (Supplemental Figure 7).[47] Sanding was utilized as a test model, as it would produce a particulate exposure with the greatest potential for inhalation.

Company 1 used an acrylonitrile butadiene styrene matrix with incorporation of 3% by weight of their PC-MW (Figure 1). Company 2 used a glass fiber epoxy resin laminate with 0.15% incorporation by weight (Figure 1). Sanding resulted in an aerosol consisting of particulates with protrusions representative of the percent CNT incorporation (Figure 8a,b). No free MWCNTs were observed from either composite containing PC-MW following electron microscopy evaluation.[47] The size distribution analysis of the particulate aerosol indicated a shift in the particle count for company 1 to produce smaller particles (a leftward shift; Figure 8c), which was not attributable to sandpaper abrasive particles. This was observed with different types of sandpaper[47] and previously with increasing percent incorporation of CNTs.[43] In contrast, size distribution curves for particle count and mass concentration of the sanded composites from company 2 were similar in profile (Figure 8d,f). Additionally, the base matrices used in this study affect aerosol generation (*e.g.*, particles/cm^3) and composition (*e.g.*, % of aerosol that is degraded sandpaper).[47] Glass fiber epoxy resin laminate produces greater particle number and respirable mass concentrations compared to acrylonitrile butadiene styrene. Also the glass fiber resin laminate is a harder material, and more of the aerosol is from sandpaper grit. Collectively, these results demonstrate the percent incorporation of MWCNTs, as well as the matrix chosen, will affect the aerosol generated following industrial sanding scenarios. Similar conclusions have been reached following weathering of nanoenabled composites.[48]

The respirable fraction of the composite aerosol generated from sanding was collected for *in vivo* toxicity evaluations. Exposure to the respirable fraction from company 1 PC-MW-enabled composite particulate acutely increased cytotoxicity and pulmonary inflammatory gene expression in comparison to the neat composite (Figure 8g,i; Supplemental Table 9). Protein levels of Ccl2 and Ccl22 measured in the bronchoalveolar lavage fluid were also significantly elevated in the PC-MW-enabled composite compared to the neat composite (Supplemental Table 9). The panel of altered mediators suggest enhanced macrophage activation. At the dose administered there was no influx of polymorphonuclear cells (Supplemental Table 8) or increased protein expression of the neutrophil chemoattractant Cxcl2 (Supplemental Table 9). Since mice were dosed on an equal mass basis, the ultrafine particle shift in the PC-MW-enabled composite aerosol, a secondary effect of PC-MW incorporation, was a potential contributing factor to the increased acute toxicity. Also, 60% of the particles generated by the fine sandpaper had PC-MW protrusions at a rate of 3.65 protrusions per particle.[47] Potential exists for an altered acute macrophage response to particles with PC-MW protrusions compared to the particles without.

There was generally no difference in pulmonary inflammation (Figure 8h,j; Supplemental Tables 8 and 9) by equal mass exposures for company 2, which was expected given the similar profile of the size distribution curves. The results from company 2 complement previous work showing no enhanced toxicity with size distribution curves having similar profiles.[46,49] It should be noted that while toxicity was not different with company 2, the PC-MW-enabled composite generated a reduced respirable mass concentration in comparison to the neat composite when subjected to a similar sanding protocol.

In summary, as-produced MWCNT exposure warrants proper evaluation and effective management. By coating MWCNTs with polymers, the improved ease in handling, potential to reduce dustiness, and use of less material can reduce possible exposures. Companies have made available CNTs preformulated in different matrices, limiting dry powder handling. We emphasize the importance of this workplace-representative approach to provide the most relevant context for potential human health outcomes. Given the diversity of engineered nanomaterials, especially within a single class, linking ongoing exposure assessment to toxicology experimental design is immensely useful and critical. The initiative and responsibility of the participating companies illustrates the beneficial nature of communication between advanced material scientists and toxicologists. The use of engineered nanomaterials in conventional and advanced manufacturing technologies, such as additive manufacturing, is becoming an everyday reality, and the assessment of toxicity should encompass perspectives beyond the as-produced material.

CONCLUSION

In conclusion, and not unexpectedly,[2] toxicity was induced by as-produced MWCNTs. Exposures depositing primarily in the conducting airways have the possibility to induce bronchiolitis obliterans. The intermediate step of polymer coating itself can attenuate toxicity. Additionally, the polymer coating exhibited stability and may alter how the lung recognizes MWCNTs. PC-MW incorporation into specific composites can affect the aerosol generated during mechanical processing and, in certain scenarios, alter acute toxicity. Importantly, no free MWCNTs were observed from sanded composites, consistent with previous work suggesting <4% loading by mass did not result in release of free CNTs.[43] Overall, as MWCNT handling transitions from dry powder to an end product, the number of workers and potential consumers along the life cycle increases, but toxicity and/or potential for exposure to as-produced materials may greatly diminish.

MATERIALS AND METHODS

Materials. Multiwalled carbon nanotube (MWCNT)-based materials used in this study were generously provided by two companies within the United States. Each company provided an as-produced MWCNT (AP-MW), a polymer-coated MWCNT (PC-MW), and composite samples that were neat (no PC-MW) or contained PC-MW at the specified mass percent (Figure 1). The AP-

DOI: 10.1021/acsnano.7b03038
ACS Nano 2017, 11, 8849−8863

MW produced by company 1 was manufactured to be highly entangled cross-linked MWCNTs. The AP-MW was surface coated by an aqueous spray process designed to apply a specific amount of solubilized polyurethane and then dried to remove excess moisture. The PC-MW was utilized in an acrylonitrile butadiene styrene composite at 3% by mass. Company 2 used Arkema Graphistrength C100 for their AP-MW. The AP-MW was conjugated with a proprietary poly(arylene ethynylene) coating by π-stacking. The polymer backbone was adsorbed along the side walls of the tubes with organic side chains attached to the backbone of the polymer. The coating is similar, but not exactly the same, as the conjugated polymer described by Chen *et al.*.[34] The PC-MW was utilized in a glass fiber epoxy resin laminate composite at 0.15% by mass. The polymers are soluble in 1−10 mg/mL of solvent.

Characterization. *Length and Diameter.* A protocol was established for the measurements of diameter and length of MWCNTs using a high-resolution field emission scanning electron microscope with scanning transmission electron microscopy capabilities (FESEM/STEM, S-5500, Hitachi High Technologies America, Schaumburg, IL). The samples were prepared by adding a portion of the MWCNT material into a glass vial containing isopropyl alcohol and sonicating for approximately 5 min. A TEM grid was then dipped into the suspension, producing a well-dispersed sample. Initially, a low magnification was used (~5−10k×) to locate MWCNTs. Once a MWCNT was located, the magnification was increased appropriately to measure width and length. Using the measuring tools of the electron microscope's software (FE-PC SEM, Ver. 2.8, Hitachi High Technologies America), straight lines were manually drawn to connect the distances to be measured. For length measurements, the longest straight line was drawn between two extremities of a fiber without following the curvatures of the fiber. For the diameter, measurements were taken drawing a straight line of the distance perpendicular to the fiber's walls. High-resolution images of the CNTs were collected on a 200 kV dedicated scanning transmission electron microscope (HD-2300A, Hitachi High Technologies America, Schaumburg, IL).

Two-Dimensional Agglomerate Sizing. AP-MW and PC-MW were prepared in physiologic dosing media and prepared for analysis using a field emission scanning electron microscope (FESEM; Hitachi S-4800, Tokyo, Japan). The largest crosswise diameter of 75 agglomerates was measured for each material.

X-ray Photoelectron Spectroscopy. MWCNT samples were placed on two-sided tape for X-ray photoelectron spectroscopy (K-Alpha XPS, Thermo Scientific, Waltham, MA). High-resolution scans of carbon and oxygen were made and the main carbon peak was shifted to a binding energy of 284.5 eV for consistency between samples.

Raman Spectroscopy. Raman spectra of the MWCNT samples were generated using a Horiba LabRAM HR800 (Horiba Instruments, Edison, NJ), equipped with an optical microscope, a confocal aperture of 200 μm, a 1024 × 256 pixel Synapse CCD detector, and a 600 grooves/mm grating. The spectral resolution of this instrumental configuration is 2.4 cm^{-1}. Light from a 473 nm argon laser was focused onto the sample using a 100× long-working distance objective. A neutral density (ND) filter was placed in the beam path that permitted 10% of the maximum laser power to pass, such that approximately 470 μW was at the sample. Each analyte was measured using a 5-s acquisition time and two accumulations. Four unique sample locations were evaluated, and these spectra were averaged into one representative Raman spectrum per sample. The exception to these acquisition parameters was the reference polymer used to encapsulate the MWCNT from company 2 as intrinsic sample fluorescence obscured Raman vibrational modes. This sample was measured with a 633 nm helium−neon laser, 600 grooves/mm grating, 100× long-working distance objective, 100 μm confocal aperture, 10 s acquisition time with three accumulations, and a ND filter that only permitted 1% of the maximum laser power to reach the sample. The Raman spectra were baseline-corrected and averaged using the LabSpec 6 software package.

ζ-Potential. All measurements for ζ-potential, an indicator of particle surface charge in the medium, were performed using a Nano ZS90 instrument (Malvern Instruments, UK). Viscosity of control medium was previously determined at room temperature using a VS-10 viscometer (Malvern Instruments) and used as the value for calculation of ζ-potential.

Endotoxin. The endotoxin contamination was measured using the Limulus Amebocyte Lysate test.

Metal Analysis. Metal content was measured by inductively coupled plasma atomic emission spectroscopy. Samples were digested using a microwave digestion system (MARS, CEM). Five milligrams of each sample was added to the digestion vessel, followed by 10 mL of concentrated nitric acid. The samples were then digested using the following program: maximum power 400, 100% power, ramp 20 °C/min, 600 psi, temperature 230 °C, hold time 60 min. After digestion, the samples were heated on a hot block to reduce the volumes to about 1 mL, and the volumes were then adjusted to 10 mL using deionized water. Sample digests were analyzed according to NMAM 7300.

Surface Area. Surface area was measured using Brunauer−Emmett−Teller (BET) methodology. Samples were degassed in ultrahigh purity (UHP) nitrogen for 30 min at 90 °C and then for 90 min at 200 °C. The specific surface areas were determined by a five-point BET measurement with UHP nitrogen as the adsorbate and liquid nitrogen as the cryogen. The following relative pressures (P/P^0) were used: 0.05, 0.10, 0.15, 0.2, and 0.25.

Density. Bulk density of each MWCNT material was determined based on ISO 23145. Briefly, a 10 mL graduated cylinder was tared on a calibrated analytical balance, MWCNT was added, and the container gently tamped to level the powder. The volume of the powder was recorded to the nearest 0.1 mL, and the cylinder with powder was reweighed. Density was calculated as the mass of powder divided by volume. Three replicate samples were drawn per MWCNT material and the results expressed as means ± standard deviation.

Dustiness. Dustiness was measured using the Venturi dustiness device as previously described.[22] Dustiness, a unitless measure (mass/mass), was represented as a percentage of total and respirable airborne mass collected to the quantity of test powder prior to dispersion.

Stability of Polymer Coating in Biological Fluids. PC-MW from each company were incubated in artificial lysosomal fluid (ALF) or interstitial fluid (Gamble's).[50] PC-MW was incubated at a concentration of 500 μg/mL for 1 and 21 days for ALF and 21 days for Gamble's. Samples were placed in an incubator and maintained at 37 °C under constant rotation (60 rpm). Following 1 or 21 days of incubation, PC-MW were washed three times with deionized water. Following the last wash, PC-MW were removed and allowed to dry prior to analysis by Raman spectroscopy and X-ray photoelectron spectroscopy.

Animals. Male C57BL/6J pathogen-free mice weighing 20−25 g were obtained from Jackson Laboratories (Bar Harbor, ME). All mice were housed in the Association for Assessment and Accreditation of Laboratory Animal Care (AAALAC)-accredited NIOSH animal facility and afforded food and tap water *ad libitum* in ventilated cages, on autoclaved hardwood chip bedding and an environment of controlled humidity, temperature, and 12:12 light/dark cycles. Animals were allowed to acclimate for at least 7 days prior to use in any experiments. Animal care and use procedures were conducted in accordance with the "PHS Policy on Humane Care and Use of Laboratory Animals" and the "Guide for the Care and Use of Laboratory Animals" (2011). The procedures utilized in this study were approved by the National Institute for Occupational Safety and Health Institutional Animal Care and Use Committee.

Study Design. Male C57BL/6J mice, 8 to 10 weeks of age, were exposed by oropharyngeal aspiration to either vehicle (physiologic dosing medium; DM), AP-MW, or PC-MW at two different concentrations (n = 6 mice per group). Low (4 μg) and high (40 μg) doses were chosen from previous studies based on exposure assessment.[1,14] The lowest dose was chosen to reflect relevant human exposure levels of the MWCNT industry to date, whereas the high dose is known to induce pulmonary pathology.[1,14] According to the manufacturers, the polymer coatings were 7 and 15% of the total weight from company 1 and company 2, respectively. The weight of the coating was accounted for to dose by equal mass of MWCNT.

DOI: 10.1021/acsnano.7b03038
ACS Nano 2017, 11, 8849−8863

Mice were sacrificed at 1, 7, 28, and 84 days postexposure to analyze pulmonary inflammation, regional distribution of particles, and histopathological changes.

One set of mice (n = 6 mice per group) was used to collect bronchoalveolar lavage (BAL) by standard procedures.[4] The acellular fraction was used for cytotoxicity measurements and protein analysis (RodentMAP v.3.1; Myriad RBM, Austin, TX). For some proteins measured, analyte levels were below the level of detection (*e.g.*, vehicle exposures) but measurable for other groups (*e.g.*, 40 μg exposure groups). In these instances, values below the level of detection were added as 50% of the limit of quantification and analysis was done using non parametric tests as indicated in the Statistics section. The cellular fraction was used for total cell count using a hemocytometer and determining differentials. A second set of mice (n = 6 mice per group) was used for gene expression changes and histopathology analysis. Following exsanguination, the left lung lobe was ligated, removed, and frozen at −80 °C for gene expression analysis as previously described.[14] The right lobes were inflated with 10% buffered formalin by gravity fixation.

In parallel studies, male C57BL/6J mice, 8 to 10 weeks of age, were exposed by oropharyngeal aspiration to either vehicle, respirable particles from composites without PC-MW, or respirable particles from the same composites containing PC-MW. Complete details of composite particle generation and characterization, the sampling protocol, associated data analysis, and collection of respirable particles are detailed in subsequent sections. A single dose of 40 μg was used and is in direct comparison to doses used previously for composite dusts.[46] Mice were euthanized at 1, 28, and 84 days postexposure to evaluate pulmonary cytotoxicity, inflammation, and histopathological changes. As above, two sets of mice were studied (n = 6 mice per group for each set).

Facility Representative Material Preparation and Dosing. *Personal Breathing Zone (PBZ).* Samples were collected on 25 mm mixed cellulose ester filters (0.8 μm pore size; SKC Inc., Eighty Four, PA) using Leland Legacy pumps (SKC Inc.) operating at 5 lpm. The transmission electron microscopy (TEM) samples were then analyzed on a JEOL2100F TEM (JEOL USA, Inc., Peabody, MA) using a modified NMAM 7402.[18] The representative electron microscopy images of PBZ samples collected from both workplaces were used in order to determine proper dosing for the rodent model.

Material Preparation. DM was prepared fresh and contained mouse serum albumin (0.6 mg/mL) and 1,2-dipalmitoyl-*sn*-glycero-3-phosphocholine (DPPC; 0.01 mg/mL) prepared in United States Pharmacopeia (USP)-grade phosphate-buffered saline (PBS) without calcium and magnesium. Samples were sonicated for 5 min at the highest setting using an external sonicator (Hielscher Ultrasound Technology) and then 5 min using a Branson Sonifier 450 probe sonicator set to the lowest setting (10% duty cycle; output control of 1). These settings and times were determined to best mimic collected PBZ samples by comparisons of TEMs from field studies and material preparations.

Oropharyngeal Aspiration. Dosing using the well-established oropharyngeal aspiration method[51] was a necessity. The goal was to expose animals with a facility-representative particle. Company 1 in particular manufactures an agglomerated material from which <10% of the inhalable fraction is respirable, based on exposure assessment studies.[18] It was clear from TEM images from PBZ and test sample preparations that to mimic the workplace setting, inhalation exposure would not be feasible in a rodent model. Anatomically, upper airways in the obligate nasal breathing rodent are much smaller than humans and pulmonary deposition would have been minimal and not representative. By using oropharyngeal aspiration, we achieved significant conducting airway deposition and, to a lesser degree, alveolar deposition that was consistent with exposure assessment studies.

Histopathology. At sacrifice, lungs were inflated with 10% buffered formalin, processed into paraffin blocks, sectioned at 5 μm, and stained with hematoxylin and eosin (H&E). H&E-stained slides were examined by a veterinary pathologist using bright field microscopy for evaluating morphologic changes, and by polarizing light microscopy for identifying composite particles. The severity of lung pathology was scored using the following criteria: 1 = minimal, 2 = mild, 3 = moderate, 4 = moderately severe, and 5 = severe. Photomicrographs were captured using an Olympus BX53 microscope equipped with a DP73 camera.

Regional Pulmonary Distribution. For each animal, one H&E-stained section of lung was examined using the 10× objective for particle deposition. Each focus of deposition was scored individually, and was given a score from 1 to 4 based on the relative amount of particle/size of the deposit. Deposition scoring was 1 = minimal deposition/small deposit (this included individual or small clumps of particle-containing macrophages, or very small extracellular deposits of particles); 2 = minimal deposition; 3 = moderate deposition; 4 = extensive deposition/very large deposit (this included airways containing large tangles of particles or large extracellular agglomerates of particles). Individual scored deposits were tabulated based on regional distribution within the lung and included bronchiole, terminal bronchiole, alveolar duct, and alveolus. Regional deposition was expressed as a percent of the total particle burden for each region.

Micronucleus Assay. Immortalized human bronchial epithelial cells (BEAS-2B; ATCC, Manassas, VA) and primary human small airway epithelial cells (SAEC; Lonza, Walkersville, MD) were grown on two-well glass chamber slides (Nunc, Rochester, NY). Three independent experiments were performed for each exposure for SAEC and BEAS-2B cells. BEAS-2B cells were cultured in Dulbecco's modified Eagle medium supplemented with 10% serum (Invitrogen, Grand Island, NY) and 1% antibiotic-antimycotic (Corning, Corning, NY). SAEC cells were cultured following manufacturer's directions and using Cabrex media (Lonza). Once cells were 70% confluent, they were treated with 2.4 μg/mL MWCNT suspended in media, 3.2 μg/mL vanadium pentoxide (Sigma, St. Louis, MO) as positive control, or PBS (Sigma-Aldrich, St. Louis, MO) as negative control. The BEAS-2B cells were exposed for 24 h, whereas the SAEC cells were exposed for 72 h, to account for the difference between cell types regarding mitotic index. After this time, the treatment was removed and the slides were washed with PBS. The cells were fixed with ice-cold methanol for 30 min and then hybridized with Star*FISH human chromosome pancentromeric probe labeled with FITC (Cambio, Cambridge, UK) and counterstained with DAPI (Vector, Burlingame, CA). The cells were imaged using a laser scanning confocal microscope (LSM 780, Carl Zeiss MicroImaging Inc., Thornwood, NY). Photographs of a minimum of 100 cells per slide were taken and the number of micronuclei present was recorded; experiments were repeated three times for a total of 300 cells for each treatment and dose. Presence of pancentromeric probe in the micronuclei was analyzed by two independent observers. The number of centromere positive cells was recorded and measured as a percentage of total micronuclei.

Particle Agglomeration in Bronchoalveolar Lavage Fluid. To determine if AP-MW and PC-MW particles from company 2 in BAL fluid would exhibit differences in their properties, prepared materials in DM were further incubated in mouse BAL fluid. Unbound BAL fluid was separated from the material-lung surfactant corona, and analyzed by TEM. BAL fluid was obtained from mice and incubated with materials prepared for *in vivo* dosing (100 μL of BAL fluid with 50 μL of MWCNT from a stock concentration of 0.8 mg/mL) and incubated at 4 °C for 1 h. The suspensions were centrifuged at 10 000 rcf for 10 min to separate unbound BAL fluid from the CNT−surfactant corona. The supernatant was decanted and the pellet was washed three times (10 000 rcf for 10 min) using 1 mL of PBS. The pellet was resuspended in 50 μL of PBS and analyzed using TEM.

Composite particle generation, composite particle characterization, sampling protocol, and composite data analysis are summarized below and adapted from previously published methods.[47]

Composite Particle Generation. A belt sander (model 97181, Central Machinery, Camarillo, CA) was modified by removing the motor and locating it outside the generation chamber. The drive axle of the motor was connected to a pulley through a v-belt. Inside the chamber, the pulley was connected to the shaft of the belt sander. An exhaust port extracted air at a flow rate of 18 l/min while HEPA filters

DOI: 10.1021/acsnano.7b03038
ACS Nano 2017, 11, 8849−8863

were placed at the air intake ports. The sample materials were pushed toward the sanding belt by a gravity-fed carriage located above the sander. The gravity-fed carriage consisted of a vertical carriage loader with a 25 g weight at the top that served as the constant downward force. The cross-sectional area of the composite on the sanding belt was 3.0 cm^2 indicating the pressure applied was 0.082 N/cm^2. The sander was equipped with a 10.2 cm by 91.4 cm (4 in. by 36 in.) sanding belt operating at a constant speed of 5.6 m/s. A silicon−aluminum based sandpaper (R228, Norton, Saint-Gobain Abrasives, Inc., Worcester, MA) was used during the sanding process; the grit size of the sandpaper was fine (P320).

Composite Particle Characterization. Real-time, direct read instruments (DRIs) were located outside the chamber and drew the particle-laden aerosol through sampling lines. The inlets of the sampling lines were positioned at 20 cm from the belt sander and the length of the lines was 90 cm. A scanning mobility particle sizer (SMPS, model 3080, TSI, Inc., Shoreview, MN) at a flow rate of 0.6 l/min was used to measure particle number concentrations and mass concentrations ranging from 10.4 to 406.8 nm. An optical particle counter (OPC, model 1.109, Grimm Technologies, Atlanta, GA) at a flow rate of 1.2 l/min was used to measure particle number and mass concentration ranging from 0.25 to 32 μm. The total number concentration of particles from 0.004 to 3 μm was measured using a condensation particle counter at a flow rate of 1.5 l/min (CPC, model 3775, TSI).

Samples for microscopy analysis were collected using a three-piece, 25 mm cassette with a 0.4 μm polycarbonate (PC) filter connected to a sampling pump (SKC Inc., Eighty Four, PA) operating at 1.5 l/min. Additionally, a thermophoretic sampler (TPS100, RJ Lee Group, Monroeville, PA) collected particles directly on a TEM grid at a flow rate of 0.05 l/min. A collection boat made of aluminum foil was placed under the belt sander to collect particle debris from the sanding process.

The filter samples and TPS100 samples were manually examined in a high-resolution field emission scanning electron microscope with scanning transmission electron microscopy capabilities (FESEM/STEM, S-5500, Hitachi High Technologies America, Schaumburg, IL). The primary objective was to identify both unbound and protruding PC-MW in the composite particles.

Sampling Protocol. Background measurements inside the sampling chamber were taken for 5 min with the DRIs when the belt sander was off (no sanding occurred). During background measurements, the TPS100 and the filter's sampling pump were off. Following the background measurements, the belt sander was turned on and allowed to warm for 30 s, and the gravity-fed carriage was then operated to lower the sample toward the sander. The TPS100 and sampling pump were activated when the sanding started. Particle concentrations inside the chamber were allowed to stabilize for 8 min after which measurements were recorded with the DRIs for 7 min. Following the sampling period, the sample was lifted, the belt sander was turned off, the sandpaper was replaced with a new band of the same grit type, and the experiment was repeated. Each material was tested in triplicate.

Each sampling period lasted a total of 20 min, which was broken down into 5 min of background concentration measurements where no sanding took place, 8 min of sanding to ensure stabilization of the generation of particles, and another 7 min of sanding for particle measurements. The TPS100 and filter cassette were active for the 15 min of sanding. One cumulative TPS100 sample was collected for all three repetitions with the same sandpaper grit, while the filter cassettes were replaced before each repetition. The DRIs were active during the 5 min of background measurements and during the 7 min sanding after the stabilization period. The belt sander was disassembled and the cabinet cleaned with a vacuum and wiped with wet wipes when switching between test sample types. Field-blank tests were taken to ensure that no cross-contamination occurred between samples. During the field-blank tests all protocols of a regular trial were followed with the exception that no material was fed to the sander.

Composite Data Analysis. The data from the DRIs were averaged from the triplicate runs for each material. Background measurements were subtracted from the final measurements to account for background concentrations. Particle number concentrations were obtained from the OPC and CPC measurements. The particle size distribution graphs were obtained from the OPC and SMPS measurements. The midpoint diameter channels that ranged from 10.4 to 283.9 nm were used from the SMPS, while the midpoint diameter channels that ranged from 300 nm to 32,000 nm were used from the OPC. Values were averaged from the triplicate runs for each material. The DRIs' background values were subtracted from the final measurement values.

Respirable Particle Collection from Sanded Composites. Respirable particles were separated from the sanding particles using a stainless steel cyclone (URG-2000-30EM, URG Corp., Chapel Hill, NC) operated at 30 lpm. At this flow rate the cyclone provides a cutpoint diameter of approximately 4.5 μm. A polycarbonate membrane filter (Isopore GTTP14250, Millipore, Billerica, MA) with 0.2 μm pore size and 10 cm (4 in.) diameter was placed at the outlet of the cyclone. The filter was then brushed with a clean brush and the collected particles were placed in sterile centrifuge tubes. The procedure was repeated until at least 10 mg of respirable particles were collected for each material.

Statistics. The analysis of data from this study utilized SAS/STAT software, Version 9.4 of the SAS system for Windows (SAS Institute, Cary, NC). Generally, we utilized PROC MIXED to run a two-way factorial analysis of variance with treatment and time as the independent variables. Pairwise comparisons where appropriate were obtained from the overall analysis using the "pdiff" option. In situations where there were not multiple days of measures, a one-way ANOVA was utilized with treatment as the independent variable. For variables where the assumptions of the analysis were not met, such as heterogeneous variance, the data were log-transformed and reanalyzed. If the assumptions were still not met, then data were analyzed using nonparametric Kruskal−Wallis tests for each postexposure time point, and pairwise comparisons were generated using the Dwass, Steel, Critchlow−Fligner method. The Kolmogorov−Smirnov two-sample test was used to compare the length distributions from the coated and uncoated nanotubes for each company. These comparisons were performed using JMP v12.1 (SAS Institute). All differences were considered significant at $p < 0.05$.

ASSOCIATED CONTENT

Supporting Information

The Supporting Information is available free of charge on the ACS Publications website at DOI: 10.1021/acsnano.7b03038.

Additional tables containing raw data of cellular analysis of collected bronchoalveolar lavage, protein determinations, and histopathology scoring (PDF)

Additional figures of material characterization and toxicity (PDF)

AUTHOR INFORMATION

Corresponding Author

*Tel: 304-285-5903. Fax: 304-285-5708. E-mail: efi4@cdc.gov.

ORCID

Aaron Erdely: 0000-0002-2557-1673

Notes

The findings and conclusions in this report are those of the author(s) and do not necessarily represent the views of the National Institute for Occupational Safety and Health.

The authors declare no competing financial interest.

ACKNOWLEDGMENTS

The authors would like to thank N. Matin and L. Turkevich for their invaluable assistance in performing the dustiness tests on the materials. This work was funded by the Nanotechnology

DOI: 10.1021/acsnano.7b03038
ACS Nano 2017, 11, 8849−8863

Research Center of the National Institute for Occupational Safety and Health.

REFERENCES

(1) Erdely, A.; Dahm, M. M.; Schubauer-Berigan, M. K.; Chen, B. T.; Antonini, J. M.; Hoover, M. D. Bridging the Gap between Exposure Assessment and Inhalation Toxicology: Some Insights from the Carbon Nanotube Experience. *J. Aerosol Sci.* **2016**, *99*, 157−162.

(2) Oberdorster, G.; Castranova, V.; Asgharian, B.; Sayre, P. Inhalation Exposure to Carbon Nanotubes (Cnt) and Carbon Nanofibers (Cnf): Methodology and Dosimetry. *J. Toxicol. Environ. Health, Part B* **2015**, *18*, 121−212.

(3) Aragon, M. J.; Topper, L.; Tyler, C. R.; Sanchez, B.; Zychowski, K.; Young, T.; Herbert, G.; Hall, P.; Erdely, A.; Eye, T.; Bishop, L.; Saunders, S. A.; Muldoon, P. P.; Ottens, A. K.; Campen, M. J. Serum-Borne Bioactivity Caused by Pulmonary Multiwalled Carbon Nanotubes Induces Neuroinflammation Via Blood-Brain Barrier Impairment. *Proc. Natl. Acad. Sci. U. S. A.* **2017**, *114*, E1968−E1976.

(4) Erdely, A.; Hulderman, T.; Salmen, R.; Liston, A.; Zeidler-Erdely, P. C.; Schwegler-Berry, D.; Castranova, V.; Koyama, S.; Kim, Y. A.; Endo, M.; Simeonova, P. P. Cross-Talk between Lung and Systemic Circulation During Carbon Nanotube Respiratory Exposure. Potential Biomarkers. *Nano Lett.* **2009**, *9*, 36−43.

(5) Grosse, Y.; Loomis, D.; Guyton, K. Z.; Lauby-Secretan, B.; El Ghissassi, F.; Bouvard, V.; Benbrahim-Tallaa, L.; Guha, N.; Scoccianti, C.; Mattock, H.; Straif, K. International Agency for Research on Cancer Monograph Working, G. Carcinogenicity of Fluoro-Edenite, Silicon Carbide Fibres and Whiskers, and Carbon Nanotubes. *Lancet Oncol.* **2014**, *15*, 1427−1428.

(6) Kasai, T.; Umeda, Y.; Ohnishi, M.; Mine, T.; Kondo, H.; Takeuchi, T.; Matsumoto, M.; Fukushima, S. Lung Carcinogenicity of Inhaled Multi-Walled Carbon Nanotube in Rats. *Part. Fibre Toxicol.* **2016**, *13*, 53.

(7) Lam, C. W.; James, J. T.; McCluskey, R.; Hunter, R. L. Pulmonary Toxicity of Single-Wall Carbon Nanotubes in Mice 7 and 90 Days after Intratracheal Instillation. *Toxicol. Sci.* **2004**, *77*, 126−134.

(8) Mercer, R. R.; Scabilloni, J. F.; Hubbs, A. F.; Wang, L.; Battelli, L. A.; McKinney, W.; Castranova, V.; Porter, D. W. Extrapulmonary Transport of Mwcnt Following Inhalation Exposure. *Part. Fibre Toxicol.* **2013**, *10*, 38.

(9) Mitchell, L. A.; Lauer, F. T.; Burchiel, S. W.; McDonald, J. D. Mechanisms for How Inhaled Multiwalled Carbon Nanotubes Suppress Systemic Immune Function in Mice. *Nat. Nanotechnol.* **2009**, *4*, 451−456.

(10) Poland, C. A.; Duffin, R.; Kinloch, I.; Maynard, A.; Wallace, W. A.; Seaton, A.; Stone, V.; Brown, S.; Macnee, W.; Donaldson, K. Carbon Nanotubes Introduced into the Abdominal Cavity of Mice Show Asbestos-Like Pathogenicity in a Pilot Study. *Nat. Nanotechnol.* **2008**, *3*, 423−428.

(11) Ryman-Rasmussen, J. P.; Cesta, M. F.; Brody, A. R.; Shipley-Phillips, J. K.; Everitt, J. I.; Tewksbury, E. W.; Moss, O. R.; Wong, B. A.; Dodd, D. E.; Andersen, M. E.; Bonner, J. C. Inhaled Carbon Nanotubes Reach the Subpleural Tissue in Mice. *Nat. Nanotechnol.* **2009**, *4*, 747−751.

(12) Sargent, L. M.; Porter, D. W.; Staska, L. M.; Hubbs, A. F.; Lowry, D. T.; Battelli, L.; Siegrist, K. J.; Kashon, M. L.; Mercer, R. R.; Bauer, A. K.; Chen, B. T.; Salisbury, J. L.; Frazer, D.; McKinney, W.; Andrew, M.; Tsuruoka, S.; Endo, M.; Fluharty, K. L.; Castranova, V.; Reynolds, S. H. Promotion of Lung Adenocarcinoma Following Inhalation Exposure to Multi-Walled Carbon Nanotubes. *Part. Fibre Toxicol.* **2014**, *11*, 3.

(13) Shvedova, A. A.; Kisin, E. R.; Mercer, R.; Murray, A. R.; Johnson, V. J.; Potapovich, A. I.; Tyurina, Y. Y.; Gorelik, O.; Arepalli, S.; Schwegler-Berry, D.; Hubbs, A. F.; Antonini, J.; Evans, D. E.; Ku, B. K.; Ramsey, D.; Maynard, A.; Kagan, V. E.; Castranova, V.; Baron, P. Unusual Inflammatory and Fibrogenic Pulmonary Responses to Single-Walled Carbon Nanotubes in Mice. *Am. J. Physiol Lung Cell Mol. Physiol* **2005**, *289*, L698−L708.

(14) Erdely, A.; Dahm, M.; Chen, B. T.; Zeidler-Erdely, P. C.; Fernback, J. E.; Birch, M. E.; Evans, D. E.; Kashon, M. L.; Deddens, J. A.; Hulderman, T.; Bilgesu, S. A.; Battelli, L.; Schwegler-Berry, D.; Leonard, H. D.; McKinney, W.; Frazer, D. G.; Antonini, J. M.; Porter, D. W.; Castranova, V.; Schubauer-Berigan, M. K. Carbon Nanotube Dosimetry: From Workplace Exposure Assessment to Inhalation Toxicology. *Part. Fibre Toxicol.* **2013**, *10*, 53.

(15) Ma-Hock, L.; Treumann, S.; Strauss, V.; Brill, S.; Luizi, F.; Mertler, M.; Wiench, K.; Gamer, A. O.; van Ravenzwaay, B.; Landsiedel, R. Inhalation Toxicity of Multiwall Carbon Nanotubes in Rats Exposed for 3 Months. *Toxicol. Sci.* **2009**, *112*, 468−481.

(16) Pauluhn, J. Subchronic 13-Week Inhalation Exposure of Rats to Multiwalled Carbon Nanotubes: Toxic Effects Are Determined by Density of Agglomerate Structures, Not Fibrillar Structures. *Toxicol. Sci.* **2010**, *113*, 226−242.

(17) Porter, D. W.; Hubbs, A. F.; Mercer, R. R.; Wu, N.; Wolfarth, M. G.; Sriram, K.; Leonard, S.; Battelli, L.; Schwegler-Berry, D.; Friend, S.; Andrew, M.; Chen, B. T.; Tsuruoka, S.; Endo, M.; Castranova, V. Mouse Pulmonary Dose- and Time Course-Responses Induced by Exposure to Multi-Walled Carbon Nanotubes. *Toxicology* **2010**, *269*, 136−147.

(18) Dahm, M. M.; Schubauer-Berigan, M. K.; Evans, D. E.; Birch, M. E.; Fernback, J. E.; Deddens, J. A. Carbon Nanotube and Nanofiber Exposure Assessments: An Analysis of 14 Site Visits. *Ann. Occup. Hyg.* **2015**, *59*, 705−723.

(19) Hussain, S.; Ji, Z.; Taylor, A. J.; DeGraff, L. M.; George, M.; Tucker, C. J.; Chang, C. H.; Li, R.; Bonner, J. C.; Garantziotis, S. Multiwalled Carbon Nanotube Functionalization with High Molecular Weight Hyaluronan Significantly Reduces Pulmonary Injury. *ACS Nano* **2016**, *10*, 7675−7688.

(20) Li, R.; Wang, X.; Ji, Z.; Sun, B.; Zhang, H.; Chang, C. H.; Lin, S.; Meng, H.; Liao, Y. P.; Wang, M.; Li, Z.; Hwang, A. A.; Song, T. B.; Xu, R.; Yang, Y.; Zink, J. I.; Nel, A. E.; Xia, T. Surface Charge and Cellular Processing of Covalently Functionalized Multiwall Carbon Nanotubes Determine Pulmonary Toxicity. *ACS Nano* **2013**, *7*, 2352−2368.

(21) Mihalchik, A. L.; Ding, W.; Porter, D. W.; McLoughlin, C.; Schwegler-Berry, D.; Sisler, J. D.; Stefaniak, A. B.; Snyder-Talkington, B. N.; Cruz-Silva, R.; Terrones, M.; Tsuruoka, S.; Endo, M.; Castranova, V.; Qian, Y. Effects of Nitrogen-Doped Multi-Walled Carbon Nanotubes Compared to Pristine Multi-Walled Carbon Nanotubes on Human Small Airway Epithelial Cells. *Toxicology* **2015**, *333*, 25−36.

(22) Evans, D. E.; Turkevich, L. A.; Roettgers, C. T.; Deye, G. J.; Baron, P. A. Dustiness of Fine and Nanoscale Powders. *Ann. Occup. Hyg.* **2013**, *57*, 261−277.

(23) Burdett, G.; Bard, D.; Kelly, A.; Thorpe, A. The Effect of Surface Coatings on the Dustiness of a Calcium Carbonate Nanopowder. *J. Nanopart. Res.* **2013**, *15*, 1−17.

(24) Elgrabli, D.; Dachraoui, W.; Menard-Moyon, C.; Liu, X. J.; Begin, D.; Begin-Colin, S.; Bianco, A.; Gazeau, F.; Alloyeau, D. Carbon Nanotube Degradation in Macrophages: Live Nanoscale Monitoring and Understanding of Biological Pathway. *ACS Nano* **2015**, *9*, 10113−10124.

(25) Mercer, R. R.; Scabilloni, J. F.; Hubbs, A. F.; Battelli, L. A.; McKinney, W.; Friend, S.; Wolfarth, M. G.; Andrew, M.; Castranova, V.; Porter, D. W. Distribution and Fibrotic Response Following Inhalation Exposure to Multi-Walled Carbon Nanotubes. *Part. Fibre Toxicol.* **2013**, *10*, 33.

(26) Datsyuk, V.; Kalyva, M.; Papagelis, K.; Parthenios, J.; Tasis, D.; Siokou, A.; Kallitsis, I.; Galiotis, C. Chemical Oxidation of Multiwalled Carbon Nanotubes. *Carbon* **2008**, *46*, 833−840.

(27) Okpalugo, T. I. T.; Papakonstantinou, P.; Murphy, H.; McLaughlin, J.; Brown, N. M. D. High Resolution Xps Characterization of Chemical Functionalised Mwcnts and Swcnts. *Carbon* **2005**, *43*, 153−161.

(28) Wepasnick, K. A.; Smith, B. A.; Schrote, K. E.; Wilson, H. K.; Diegelmann, S. R.; Fairbrother, D. H. Surface and Structural Characterization of Multi-Walled Carbon Nanotubes Following Different Oxidative Treatments. *Carbon* **2011**, *49*, 24−36.

DOI: 10.1021/acsnano.7b03038
ACS Nano 2017, 11, 8849−8863

(29) Xia, H.; Song, M. Preparation and Characterization of Polyurethane−Carbon Nanotube Composites. *Soft Matter* **2005**, *1*, 386−394.
(30) Lee, J. S.; Choi, Y. C.; Shin, J. H.; Lee, J. H.; Lee, Y.; Park, S. Y.; Baek, J. E.; Park, J. D.; Ahn, K.; Yu, I. J. Health Surveillance Study of Workers Who Manufacture Multi-Walled Carbon Nanotubes. *Nanotoxicology* **2015**, *9*, 802−811.
(31) Muller, J.; Decordier, I.; Hoet, P. H.; Lombaert, N.; Thomassen, L.; Huaux, F.; Lison, D.; Kirsch-Volders, M. Clastogenic and Aneugenic Effects of Multi-Wall Carbon Nanotubes in Epithelial Cells. *Carcinogenesis* **2008**, *29*, 427−433.
(32) Barker, A. F.; Bergeron, A.; Rom, W. N.; Hertz, M. I. Obliterative Bronchiolitis. *N. Engl. J. Med.* **2014**, *370*, 1820−1828.
(33) NIOSH. Current Intelligence Bulletin 65: Occupational Exposure to Carbon Nanotubes and Nanofibers. U.S. Department of Health and Human Human Services, Centers for Disease Control and Prevention, Naitonal Institute for Occupational Safety and Health, Cincinnati, OH, 2013, DHHS (NIOSH) Publication Number 2013−2014.
(34) Chen, J.; Liu, H.; Weimer, W. A.; Halls, M. D.; Waldeck, D. H.; Walker, G. C. Noncovalent Engineering of Carbon Nanotube Surfaces by Rigid, Functional Conjugated Polymers. *J. Am. Chem. Soc.* **2002**, *124*, 9034−9035.
(35) Tabet, L.; Bussy, C.; Setyan, A.; Simon-Deckers, A.; Rossi, M. J.; Boczkowski, J.; Lanone, S. Coating Carbon Nanotubes with a Polystyrene-Based Polymer Protects against Pulmonary Toxicity. *Part. Fibre Toxicol.* **2011**, *8*, 3.
(36) Nau, G. J.; Guilfoile, P.; Chupp, G. L.; Berman, J. S.; Kim, S. J.; Kornfeld, H.; Young, R. A. A Chemoattractant Cytokine Associated with Granulomas in Tuberculosis and Silicosis. *Proc. Natl. Acad. Sci. U. S. A.* **1997**, *94*, 6414−6419.
(37) O'Regan, A. W.; Hayden, J. M.; Body, S.; Liaw, L.; Mulligan, N.; Goetschkes, M.; Berman, J. S. Abnormal Pulmonary Granuloma Formation in Osteopontin-Deficient Mice. *Am. J. Respir. Crit. Care Med.* **2001**, *164*, 2243−2247.
(38) Lin, S.; Cheng, Y.; Liu, J.; Wiesner, M. R. Polymeric Coatings on Silver Nanoparticles Hinder Autoaggregation but Enhance Attachment to Uncoated Surfaces. *Langmuir* **2012**, *28*, 4178−4186.
(39) Siegrist, K. J.; Reynolds, S. H.; Kashon, M. L.; Lowry, D. T.; Dong, C.; Hubbs, A. F.; Young, S. H.; Salisbury, J. L.; Porter, D. W.; Benkovic, S. A.; McCawley, M.; Keane, M. J.; Mastovich, J. T.; Bunker, K. L.; Cena, L. G.; Sparrow, M. C.; Sturgeon, J. L.; Dinu, C. Z.; Sargent, L. M. Genotoxicity of Multi-Walled Carbon Nanotubes at Occupationally Relevant Doses. *Part. Fibre Toxicol.* **2014**, *11*, 6.
(40) Hussain, S. P.; Harris, C. C. Inflammation and Cancer: An Ancient Link with Novel Potentials. *Int. J. Cancer* **2007**, *121*, 2373−2380.
(41) Bello, D.; Wardle, B. L.; Yamamoto, N.; Guzman de Villoria, R.; Garcia, E. J.; Hart, A. J.; Ahn, K.; Ellenbecker, M. J.; Hallock, M. Exposure to Nanoscale Particles and Fibres During Machining of Hybrid Advanced Composites Containing Carbon Nanotubes. *J. Nanopart. Res.* **2009**, *11*, 231−249.
(42) Cena, L. G.; Peters, T. M. Characterization and Control of Airborne Particles Emitted During Production of Epoxy/Carbon Nanotube Nanocomposites. *J. Occup. Environ. Hyg.* **2011**, *8*, 86−92.
(43) Huang, G.; Park, J. H.; Cena, L. G.; Shelton, B. L.; Peters, T. M. Evaluation of Airborne Particle Emissions from Commercial Products Containing Carbon Nanotubes. *J. Nanopart. Res.* **2012**, *14*.10.1007/s11051-012-1231-8
(44) Kingston, C.; Zepp, R.; Andrady, A.; Boverhof, D.; Fehir, R.; Hawkins, D.; Roberts, J.; Sayre, P.; Shelton, B.; Sultan, Y.; Vejins, V.; Wohlleben, W. Release Characteristics of Selected Carbon Nanotube Polymer Composites. *Carbon* **2014**, *68*, 33−57.
(45) Mackevica, A.; Foss Hansen, S. Release of Nanomaterials from Solid Nanocomposites and Consumer Exposure Assessment - a Forward-Looking Review. *Nanotoxicology* **2016**, *10*, 641−653.
(46) Wohlleben, W.; Brill, S.; Meier, M. W.; Mertler, M.; Cox, G.; Hirth, S.; von Vacano, B.; Strauss, V.; Treumann, S.; Wiench, K.; Ma-Hock, L.; Landsiedel, R. On the Lifecycle of Nanocomposites: Comparing Released Fragments and Their in-Vivo Hazards from Three Release Mechanisms and Four Nanocomposites. *Small* **2011**, *7*, 2384−2395.
(47) Kang, J.; Erdely, A.; Afshari, A.; Casuccio, G.; Bunker, K.; Lersch, T.; Dahm, M. M.; Farcas, D.; Cena, L. Generation and Characterization of Aerosols Released from Sanding Composite Nanomaterials Containing Carbon Nanotubes. *NanoImpact* **2017**, *5*, 41−50.
(48) Wohlleben, W.; Neubauer, N. Quantitative Rates of Release from Weathered Nanocomposites Are Determined across 5 Orders of Magnitude by the Matrix, Modulated by the Embedded Nanomaterial. *NanoImpact* **2016**, *1*, 39−45.
(49) Saber, A. T.; Mortensen, A.; Szarek, J.; Koponen, I. K.; Levin, M.; Jacobsen, N. R.; Pozzebon, M. E.; Mucelli, S. P.; Rickerby, D. G.; Kling, K.; Atluri, R.; Madsen, A. M.; Jackson, P.; Kyjovska, Z. O.; Vogel, U.; Jensen, K. A.; Wallin, H. Epoxy Composite Dusts with and without Carbon Nanotubes Cause Similar Pulmonary Responses, but Differences in Liver Histology in Mice Following Pulmonary Deposition. *Part. Fibre Toxicol.* **2016**, *13*, 37.
(50) Marques, M.; Loebenberg, R.; Almukainzi, M. Simulated Biological Fluids with Possible Application in Dissolution Testing. *Dissolution Technol.* **2011**, *18*, 15−28.
(51) Rao, G. V.; Tinkle, S.; Weissman, D. N.; Antonini, J. M.; Kashon, M. L.; Salmen, R.; Battelli, L. A.; Willard, P. A.; Hoover, M. D.; Hubbs, A. F. Efficacy of a Technique for Exposing the Mouse Lung to Particles Aspirated from the Pharynx. *J. Toxicol. Environ. Health, Part A* **2003**, *66*, 1441−1452.

DOI: 10.1021/acsnano.7b03038
ACS Nano 2017, 11, 8849−8863